Click Here for Full Article

Pathogen and chemical transport in the karst limestone of the Biscayne aquifer: 2. Chemical retention from diffusion and slow advection

Allen M. Shapiro,[1] Robert A. Renken,[2] Ronald W. Harvey,[3] Michael R. Zygnerski,[2] and David W. Metge[3]

Received 27 March 2007; revised 16 November 2007; accepted 8 April 2008; published 23 August 2008.

[1] A tracer experiment, using a nonreactive tracer, was conducted as part of an investigation of the potential for chemical and pathogen migration to public supply wells that draw groundwater from the highly transmissive karst limestone of the Biscayne aquifer in southeastern Florida. The tracer was injected into the formation over approximately 1 h, and its recovery was monitored at a pumping well approximately 100 m from the injection well. The first detection of the tracer occurred after approximately 5 h, and the peak concentration occurred at about 8 h after the injection. The tracer was still detected in the production well more than 6 days after injection, and only 42% of the tracer mass was recovered. It is hypothesized that a combination of chemical diffusion and slow advection resulted in significant retention of the tracer in the formation, despite the high transmissivity of the karst limestone. The tail of the breakthrough curve exhibited a straight-line behavior with a slope of −2 on a log-log plot of concentration versus time. The −2 slope is hypothesized to be a function of slow advection, where the velocities of flow paths are hypothesized to range over several orders of magnitude. The flow paths having the slowest velocities result in a response similar to chemical diffusion. Chemical diffusion, due to chemical gradients, is still ongoing during the declining limb of the breakthrough curve, but this process is dwarfed by the magnitude of the mass flux by slow advection.

Citation: Shapiro, A. M., R. A. Renken, R. W. Harvey, M. R. Zygnerski, and D. W. Metge (2008), Pathogen and chemical transport in the karst limestone of the Biscayne aquifer: 2. Chemical retention from diffusion and slow advection, *Water Resour. Res.*, *44*, W08430, doi:10.1029/2007WR006059.

1. Introduction

[2] Over the past 20 years there has been an increased awareness of the role of aquifer heterogeneity on chemical transport in subsurface environments. *Gelhar and Axness* [1983], *Dagan* [1984], and *Neuman et al.* [1987] published seminal works that related conceptual models of heterogeneous aquifer properties to the magnitude of parameters controlling chemical migration, in particular, the relation between the stochastic properties of hydraulic conductivity and the dispersivity. The results of these investigations considered aquifer properties of limited variability, and asymptotic expressions for the dispersivity were developed in terms of the stochastic properties of the hydraulic conductivity, which could then be incorporated into a Fickian definition of dispersion in the advection-dispersion equation.

[3] Many aquifer systems, however, exhibit extreme variability in the hydraulic conductivity in which large contrasts in the hydraulic conductivity may occur over relatively short distances. These systems are not always conducive to characterization with stochastic methods. For example, in fractured rock and carbonate aquifers, fractures, conduits, and vugs can act as preferential flow paths that conduct most of the groundwater and chemical constituents. The hydraulic conductivity of these features can vary over many orders of magnitude [*Shapiro and Hsieh*, 1998; *Mace and Hvorka*, 2000], which in combination with their complex spatial connectivity can produce highly convoluted flow paths over dimensions ranging from meters to kilometers.

[4] In addition to the void space associated with highly permeable features in fractured rock and carbonate formations, the unaltered rock matrix has intrinsic (or matrix) porosity. Various types of igneous and metamorphic rock are reported to have matrix porosity as large as 3% [*Wood et al.*, 1996], whereas sandstones, other sedimentary rocks, and some types of carbonate rocks may have larger matrix porosity [*Finley and Tyler*, 1986; *Mace and Hvorka*, 2000; *Cunningham et al.*, 2006]. The matrix porosity usually is not capable of transmitting a significant volume of fluid because of the small pore throat size and the highly tortuous nature of the void space. The matrix porosity, however, can play a significant role in chemical migration. The matrix porosity offers a fluid-filled, void space in contact with highly permeable features. Dissolved constituents in

[1] U.S. Geological Survey, Reston, Virginia, USA.
[2] U.S. Geological Survey, Fort Lauderdale, Florida, USA.
[3] U.S. Geological Survey, Boulder, Colorado, USA.

This paper is not subject to U.S. copyright.
Published in 2008 by the American Geophysical Union.

groundwater can diffuse from permeable features to the matrix porosity, or vice versa, depending on the direction of the chemical gradient.

[5] The coupled transport between permeable features and the matrix porosity in various types of rock has been recognized as being an important process in issues of waste isolation, remediation of contaminated groundwater, and the interpretation of the chemical and isotopic composition of groundwaters [*Birgersson and Neretnieks*, 1990; *Maloszewski and Zuber*, 1991; *Parker et al.*, 1994; *Shapiro*, 2001]. Mathematical models have been developed to consider the mass exchange between permeable features and an immobile fluid phase [see, e.g., *Coats and Smith*, 1964; *Maloszewski and Zuber*, 1991; *Haggerty and Gorelick*, 1995; *Field and Pinsky*, 2000]. In general, the mathematical expressions take the form of the advection-dispersion equation with terms coupling the chemical diffusion into or out of the matrix porosity.

[6] *Becker and Shapiro* [2000], *Shapiro* [2001], and *Guswa and Freyberg* [2002] hypothesized that the advection-dispersion equation may not accurately characterize chemical transport in highly heterogeneous geologic settings. A Fickian model of dispersion in the advection-dispersion equation may not accurately represent the large variability in the fluid velocity arising from the large range of the hydraulic conductivity. The large variability in the fluid velocity includes, at one end of the spectrum, slow advection that manifests itself similarly to chemical diffusion [*Shapiro*, 2001]. Chemical diffusion into the matrix porosity is still ongoing; however, that process may be masked by the magnitude of the apparent diffusion arising from slow advection.

[7] Controlled tracer tests provide valuable insight into the physical and chemical processes that control chemical migration under realistic geologic conditions. Experiments using multiple tracers with different free-water diffusion coefficients have been conducted in carbonate and fractured rock aquifers to identify the significance of advection and chemical diffusion and the appropriate conceptual model for chemical exchange between permeable features and the fluid in the rock matrix [*Garnier et al.*, 1985; *Becker and Shapiro*, 2000; *Meigs and Beauheim*, 2001; *Haggerty et al.*, 2001]. Such experiments, however, show a wide range of responses, and there is a general need for better understanding of the processes controlling chemical migration in highly heterogeneous geologic environments. This article focuses on the transport of dissolved chemical constituents in a highly heterogeneous karst aquifer, and the outcome of a controlled tracer test conducted over a distance of approximately 100 m.

[8] Quantitative tracer experiments in karst aquifers can provide the basis for hypotheses of aquifer heterogeneity and estimates of formation properties that control chemical migration [*Field*, 1999; *Goldscheider*, 2005]. Experiments between pairs of wells in karst aquifers are less frequently conducted than experiments between locations of natural aquifer recharge and discharge because of the complexity of the void space and the concern that highly permeable features in the formation may not communicate between injection and pumping locations [*Quinlan and Ewers*, 1985, 1986]. The tracer test described in this article makes use of previous testing conducted in April 2003 that identified hydraulic communication, travel time, and dilution of chemical constituents between injection and withdrawal wells in the karst limestone of the Biscayne aquifer in the Northwest well field (NWWF) in Miami-Dade County, Florida. *Renken et al.* [2008] provide an overview of the field setting, the spatial location of wells, the hydrogeology of the Biscayne aquifer, and the results of hydraulic and tracer experiments conducted in the NWWF. The interpretation of the tracer test described in this article is used to identify the significance of physical and chemical processes in a karst aquifer that control chemical migration, in particular, the roles of diffusion and slow advection on the retention of chemical constituents in the formation.

2. February 2004 Tracer Test Design

[9] The controlled tracer experiment conducted in the NWWF in February 2004 used well G-3817 as the tracer injection location in the Biscayne aquifer. Well G-3817 is approximately 97 m west of the production well, S-3164, and approximately 3 m east of the injection well used in the April 2003 tracer experiment conducted in the NWWF and described by *Renken et al.* [2008]. The results of the tracer experiment conducted in April 2003 are used for comparison with the tracer experiment described in this article. In both the April 2003 and February 2004 tracer experiments, production well S-3164 was used as the location of tracer recovery. Well S-3164 is a 1.22-m-diameter open hole to an elevation of approximately −21 m with a surface casing extending to an elevation of approximately −10.7 m. A map of the study site and the location of the injection and production wells are given by *Renken et al.* [2008].

[10] The injection well, G-3817, was drilled following the completion of the aquifer and tracer experiments conducted in April 2003, and the results of those tests were used to design the injection well and the methods of conducting the tracer experiment described here. Surface casing in well G-3817 extends from land surface to an elevation of −7.6 m, and was completed as a 0.15-m-diameter open hole to an elevation of −11.1 m. Injection well G-3817 was constructed with an open hole that intersected only the intervals of touching-vug porosity in the upper part of the Fort Thompson Formation of the Biscayne aquifer. In the Fort Thompson Formation, stratiform, touching-vug flow zones, mapped using detailed cyclostratigraphy and advanced borehole geophysical methods [*Cunningham et al.*, 2006], were identified as areally extensive features within the Biscayne aquifer responsible for the majority of groundwater flow [*Cunningham et al.*, 2006, *Renken et al.*, 2008]. The touching-vug flow zones in the open interval of the injection well, G-3817, are noted at elevations of approximately −8.8 and −10.0 m. The results of the April 2003 tracer experiment indicated that the touching-vug flow zone at approximately −10.0 m was responsible for the majority of the tracer movement, and thus, was likely to be more transmissive than the other touching-vug flow zones at greater depths in the Biscayne aquifer.

[11] The intervals of touching-vug porosity are separated by sections of the limestone that contain interparticle and separate-vug porosity [*Lucia*, 1983, 1995]. On the basis of the results of the aquifer test conducted in April 2003, the interparticle and separate-vug porosity provide aquifer storage, resulting in aquifer test responses that are analogous to

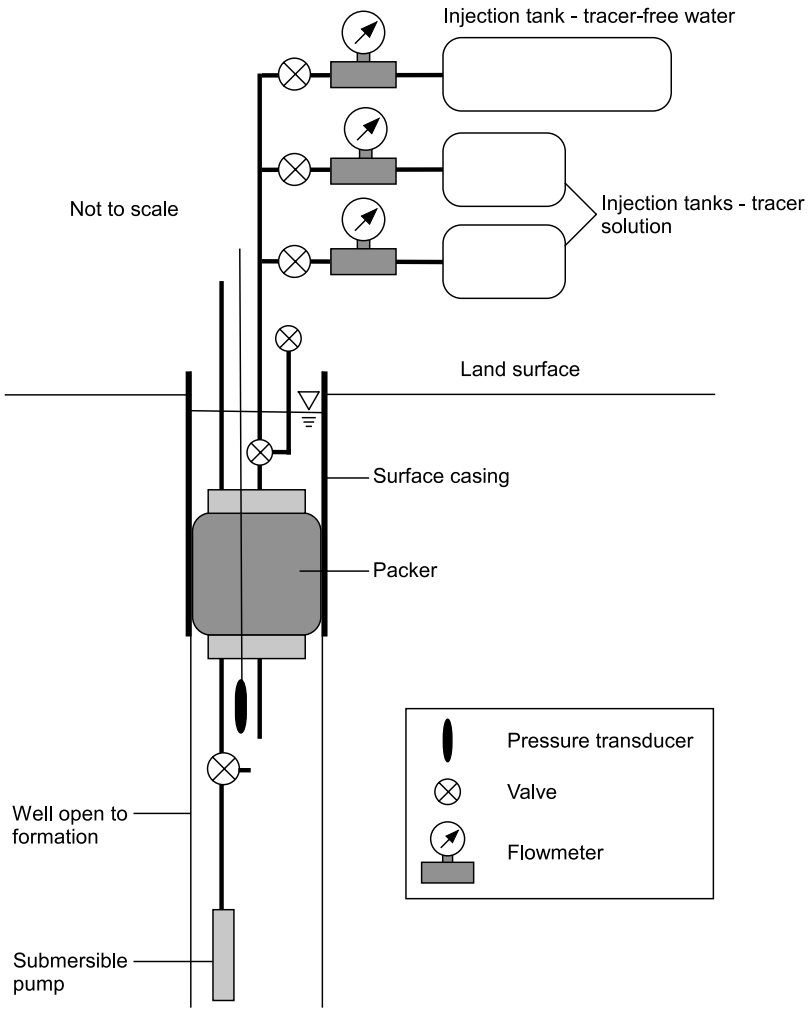

Figure 1. Apparatus used to inject the tracer solution in the injection well.

a dual-porosity aquifer [*Renken et al.*, 2008]. The average interparticle and separate-vug porosity is reported to be approximately 20%, but there is large variability in the matrix porosity due to the heterogeneous nature of the limestone [*Cunningham et al.*, 2006].

[12] The surface and down-hole apparatus used to control the injection of the tracer solutions in well G-3817 included an inflatable packer placed at the bottom of the surface casing (Figure 1). The packer reduces the volume of water in the injection interval of the borehole, and focuses the tracer solution into that portion of the well that is open to the formation. A 12.7 mm (mm) diameter tube extends through the packer to inject water into the formation from tanks at land surface. The injection tube from land surface has a valve apparatus above the packer that purges trapped air from the injection tubing prior to the tracer injection.

[13] At land surface, the injection procedure required three injection tanks. Two of the injection tanks had a capacity of approximately 189 L, and the third injection tank had a capacity of approximately 379 L. The smaller injection tanks were used to mix tracer solutions. Carboxylated polystyrene microspheres and deuterium oxide were mixed with formation water in one tank, and the second 189-L tank was used to prepare a tracer solution containing dissolved gases, in particular, sulfur hexafluoride (SF_6) and bromochlorodifluoromethane (halon-1211). The large injection tank was filled with (tracer-free) formation water, which was used to purge the injection interval after the injection of the tracer solutions. A submersible pump was used in each injection tank to pump the tracer solution into the injection well. The tubing from each submersible pump was routed through a flowmeter to monitor the rate and total volume of the injection solution. In the results of the February 2004 tracer experiment, the concentrations of deuterium (^2H) and halon-1211 at the production well did not provide acceptable signals for interpretation. Thus, only the results for SF_6 are described in the remainder of this article. *Harvey et al.* [2008] describe the results associated with the recovery of the microspheres from this experiment.

[14] The tracer solutions injected into the well had a combined density of approximately 1.010 g/cm^3, which is greater than that of the ambient groundwater. To prevent density contrasts in the injection well, a submersible pump was positioned near the bottom of the injection well and was used in conjunction with a recirculation valve located near the top of the injection interval (Figure 1). During the injection of the tracer solutions and the tracer-free water, water from the bottom of the injection interval was pumped at a low rate to the top of the injection interval in the well. The recirculation valve could also be closed to pump water

from the injection interval to land surface. This latter procedure was used to pump water from the formation for mixing the tracer solutions prior to the experiment.

[15] Prior to initiating the tracer experiment, the production well (S-3164) and other production wells in the vicinity were turned off to establish an equilibrium condition from which to start an aquifer test. The production wells in the NWWF that continued to operate and supply water to the Miami-Dade County area during the testing conducted in 2004 were the three southernmost production wells (at distances of 1213 m or more south of S-3164) and the three northernmost production wells (at distances of 914 m or more to the north) (Miami-Dade Water and Sewer Department, written communication, 2004). On 26 January 2004 (11 days prior to the start of the tracer experiment in the NWWF), production well S-3164 was started and pumped at a rate of 476 L/s and water level responses in observation wells in the NWWF were monitored. The other production wells operating in the NWWF were pumped at approximately the same rate as S-3164. The results of this aquifer test were similar to the hydraulic responses recorded by pumping the same production well (S-3164) during experiments conducted in April 2003 [*Renken et al.*, 2008]. The pumping rate in S-3164 and the other wells operating in the NWWF were maintained at a constant rate (with fluctuations of approximately ±2%) prior to and during the tracer experiment.

[16] *Renken et al.* [2008] discussed the effect that various hydrologic stresses have on groundwater flow conditions in the NWWF, in particular, the effects of precipitation and the operation of the gated control structures on the canals that surround the NWWF. During the 2004 tracer experiment, precipitation was less that 0.254 cm in areas east of the NWWF, but heavy rain showers occurred between 30 January 2004 and 1 February 2004, resulting in precipitation amounts of 4.57 to 10.1 cm at sites located north, west, and southwest of the NWWF. The precipitation caused an accompanying increase in canal stages, and the water level in an observation well (G-3772) 35 m west of the production well rose approximately 15.8 cm. The heavy precipitation occurred approximately 5 d prior to the injection of the tracer solution, and the change in the groundwater elevation dissipated after approximately 1 day because of the high transmissivity and low storativity associated with the touching-vug flow zones [*Renken et al.*, 2008]. Thus, aquifer responses to ambient hydraulic stresses were regarded as having an insignificant effect on groundwater flow conditions immediately prior to and during the tracer injection on 5 February 2004, and during the period of monitoring the tracer recovery at the production well, S-3164, which ended on 12 February 2004.

[17] On 5 February 2004, the submersible pump in the injection interval of G-3817 was used to fill the tracer injection tanks at land surface. The tank used to prepare the tracer solution containing SF_6 was designed to be pressure tight. Pressure-tight fittings were inserted into the walls of the tank to house the injection tubing and the electrical cable for the submersible pump in the tank. Approximately 30 min prior to the injection of the tracer solutions, SF_6 (prepared in pressurized canister) was bubbled through the water using multiple aquarium air diffusers placed in the bottom of the tank. The tank had a 6.35 mm diameter tube extending through a pressure-tight fitting at the top of the tank, so that the end of the tube was above the free-water surface in the tank. The other end of this tube was placed at the bottom of a 20-L bucket filled with water to maintain a positive pressure on the free-water surface of the injection tank. During the bubbling of the gas through the water in the tank, and during the injection of the tracer solution, water in the tank was agitated to facilitate equilibrium conditions between the gas in the head space of the tank and the gas in solution.

Table 1. Composition of SF_6 in Injection Solution[a]

	Value
Water temperature[b] (°C)	25
Henry's law constant for SF_6,[c] K (mol/L atm)	2.33×10^{-4}
Atmospheric pressure,[b] P (atm)	1.0081
Additional pressure applied to free-water surface,[b] P_b (atm)	0.0589
Vapor pressure,[d] P_{H2O} (atm)	0.03127
SF_6 mole fraction in air,[e] x'	0.0270
SF_6 concentration in injection solution, C^* (mol/L)	6.527×10^{-6}
Volume tracer solution injected,[b] V (L)	171.4
Quantity of tracer injected, M (mol)	1.119×10^{-3}

[a]Here °C is degrees Celsius; mol is moles; atm is atmospheres; L is liters; $C^* = K\,x'\,[(P + P_b) - P_{H2O}]$; $M = VC^*$.
[b]Measurement made during preparation or injection of the tracer solution.
[c]Henry's law constant for SF_6 from *Bullister et al.* [2002].
[d]*Plummer and Busenberg* [2000].
[e]From preparation of gases bubbled through water in the injection tank.

[18] The tracer solution was injected into well G-3817 on 5 February 2004 at 1302:00 and continued until 1321:30; 171.5 L of the tracer solution containing SF_6 were injected. This was immediately followed by the injection of 370 L of the tracer-free solution over approximately 28 min. After the injection of the tracer solution, a water sample isolated from the atmosphere was not successfully collected from the water remaining in the injection tank. The mass of the SF_6 injected into the formation was calculated using the temperature of the water, the composition of the SF_6 in the pressurized canister, and the Henry's law constant for SF_6 (Table 1). Some uncertainty exists in this calculation because of the assumption of equilibrium conditions. The effect of possibly overestimating the mass of the SF_6 in the tracer solution will be considered in the discussion of the results.

3. Water Sampling and Analysis

[19] Water samples were collected from a sampling manifold that diverted a small volume of water at the production well, S-3164. For the analysis of SF_6, water was collected through a syringe and needle that was inserted into a septum in a stainless steel fitting at the sampling manifold. Approximately 20 mL of water were drawn into the syringe and then injected through the septum of a pressure-tight sampling bottle that was prefilled with nitrogen. The bottles were weighed prior to the sample collection, and then weighed again to determine the mass and volume of water injected into the bottle. Samples were collected hourly for several hours prior to the injection of the tracer solution, and every 15 min for the first 16 h after the tracer injection. This was followed by the collection of samples every half hour for 13 h, hourly for 27 h, and every 4 h until the termination of sampling on 12 February 2004.

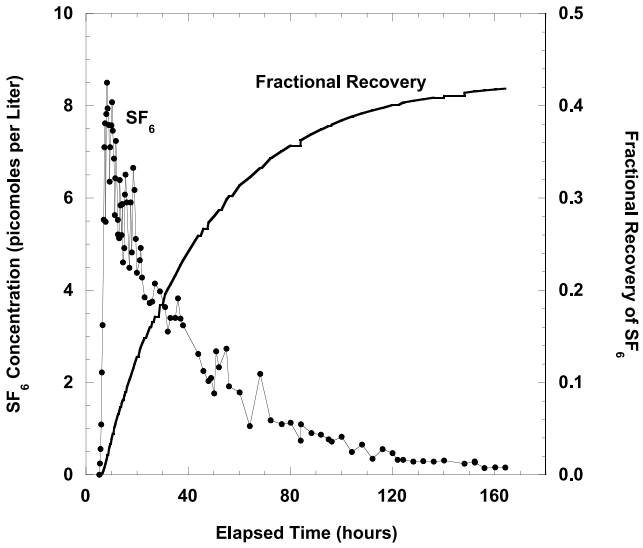

Figure 2. Concentration of SF_6 and fractional recovery of SF_6 at the tracer recovery well, S-3164, as a function of the elapsed time after the start of the tracer injection.

[20] Sample bottles were shipped to the USGS Reston (Virginia) Chlorofluorocarbon Laboratory and were analyzed for the concentration of SF_6 using gas chromatography [*Busenberg and Plummer*, 2000] approximately three weeks after collection. The gas chromatograph was calibrated with standards that ranged from 5 to 1000 parts per trillion volume (pptv) SF_6. The pressure in the sample bottle was measured and concentrations of SF_6 were corrected for the pressures above atmospheric pressure. The concentration in each sample was calculated using the combined masses of SF_6 in the head space of the sample bottle and the calculated mass of SF_6 in solution. The measured concentrations have an uncertainty of ±5% for SF_6 concentrations in the head space greater than 1 pptv, and ±10% for SF_6 concentrations in the head space less than 1 pptv.

[21] The breakthrough curve for SF_6 at the production well, S-3164, is shown in Figure 2. The first detection of SF_6 occurred at approximately 5.5 h after the start of the injection, and the peak concentration occurred at approximately 8.25 h after the start of the injection. Following the peak concentration, there is a decreasing trend in the SF_6 concentration, but it is not monotonic. The variability in the SF_6 concentration is likely the result of the error in the method of analyzing for SF_6. The breakthrough curve for SF_6 also shows an elongated tail, where the last sample with a detectable level of SF_6 occurs at approximately 164 h after the injection.

[22] Figure 2 also shows the cumulative mass recovery of SF_6 at the production well as a fraction of the mass of SF_6 injected into the formation. On the basis of the calculated mass in the injection solution (Table 1), approximately 42% of the SF_6 was recovered at the production well at the time when SF_6 was last measured above the detection limit. The trend associated with the declining limb of the breakthrough curve indicates that SF_6 was still being withdrawn at the production well; however, the SF_6 concentration was below the detection limit. The poor mass recovery could be attributed to the stripping of gases in the production well during the collection of water samples. Poor mass recovery could also be attributed to overestimating the mass of SF_6 in the injection solution under the assumption of equilibrium conditions. In the following section, evidence is given that can attribute the percentage of the mass recovery and the character of the breakthrough curve shown in Figure 2 to physical and chemical processes in the formation.

4. Comparison of April 2003 and February 2004 Tracer Tests

[23] Tracer experiments conducted with multiple tracers with different free-water diffusion coefficients provide insight into process controlling chemical migration in heterogeneous geologic environments [*Becker and Shapiro*, 2000]. Although it is advantageous to use multiple tracers with different characteristics in a single test, it is also possible to compare the results of multiple tracer tests conducted under similar conditions with different tracers [see, e.g., *Garnier et al.*, 1985; *Becker and Shapiro*, 2000, 2003]. In analyzing the breakthrough curve for SF_6 from the February 2004 tracer test, the results of the tracer test conducted in the NWWF in April 2003 using the fluorescent dye Rhodamine WT (RWT) will also be used to provide insight into the chemical and physical processes controlling chemical migration in the Biscayne aquifer.

[24] The February 2004 tracer test was conducted in the same orientation to the production well and over approximately the same distance as the April 2003 test. The injection well in the February 2004 test is approximately 3 m east of the injection well used in the April 2003 experiment, and the production well, S-3164, was used as the location of tracer recovery in both tests. In addition, the 2003 tracer test was conducted by injecting the tracer solution in well G-3773 over a 10-m-long open interval of the Biscayne aquifer, and almost 6000 L of tracer-free water was used to flush the tracer from the injection well over approximately 1 h [*Renken et al.*, 2008]. In the 2004 test, the tracer solution was injected over 3.4-m-long open interval of the Biscayne aquifer and approximately 370 L of tracer-free water was used to flush the injection interval of the well over 48 min.

[25] In the 2003 test, the tracer solution and the tracer-free fluid were distributed over multiple touching-vug flow zones over a 10-m-thick open interval in the Biscayne aquifer; however, the touching-vug flow zones immediately below the surface casing in injection well, G-3773, were shown to be responsible for the first detection and the peak concentration of the tracer in the 2003 test. These same touching-vug flow zones were isolated in the 3.4-m-long open interval of the injection well, G-3817, used in the 2004 tracer test. Consequently, the early part of the breakthrough curves from the 2003 and 2004 tests can be readily compared. The latter part of these tests, however, would not be suitable for comparison because the tracer solution in the 2003 tracer test interrogated touching-vug flow zones that were not involved in the 2004 tracer test. Also, the 2003 tracer test was terminated several hours after the peak concentration was measured in the production well, further prohibiting the comparison of the latter parts of both tests.

[26] The volume of the tracer-free water used to flush the boreholes in the 2003 and 2004 tracer tests is not considered to have a significant impact on the comparison of the results from the two tracer tests. In the 2003 tracer test, the tracer-

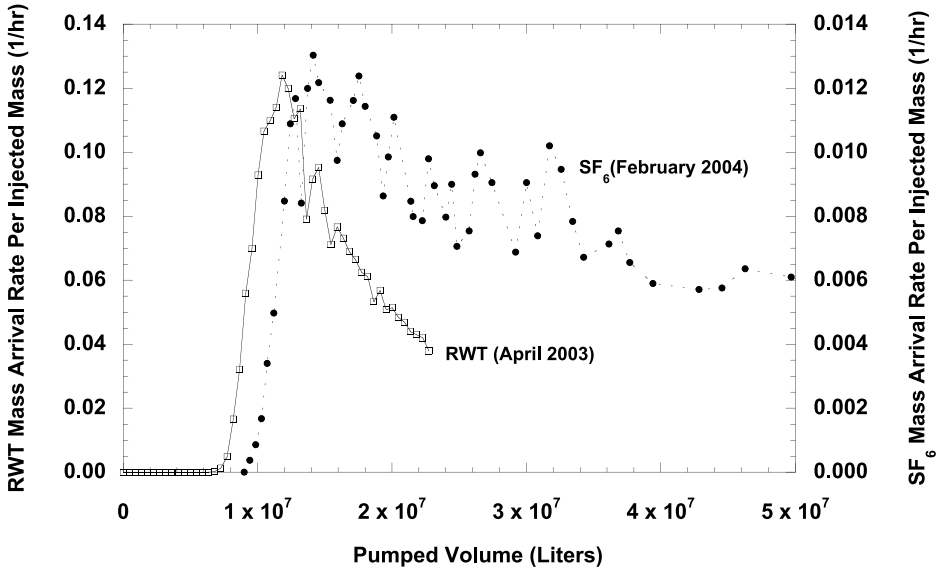

Figure 3. Concentrations of RWT from the April 2003 tracer test [*Renken et al.*, 2008] and SF_6 from the February 2004 tracer test at the tracer recovery well, S-3164, as a function of the pumped volume at the tracer recovery well.

free water was distributed over the touching-vug flow zones over the 10-m open interval of the injection well, G-3773. Thus, only a portion of the tracer-free water was introduced into the touching-vug flow zones that are consistent with the injection well used in the 2004 tracer test. Furthermore, the volume of tracer-free water used to flush the tracer solution into the formation in both the 2003 and 2004 tracer tests was similar relative to the volume of the fluid column in the injection well. In the 2004 tracer test, approximately 6 times the volume of the fluid column in the injection well was used to flush the open interval of the borehole, whereas the volume of the tracer-free water used to flush the tracer solution during the 2003 tracer test was approximately 7 times the volume of the fluid column in the injection well.

[27] Because slightly different pumping rates were used in the 2003 and 2004 tracer tests, the breakthrough curves from the two tests can be compared by plotting the breakthrough curves as a function of the cumulative pumped volume from the production well; the cumulative volume pumped is a surrogate for the elapsed time in each test. Figure 3 shows the rate of mass arrival per injected mass (cQ/M) associated with RWT from the April 2003 tracer test, and SF_6 from the February 2004 tracer test, as a function of the cumulative pumped volume; where the rate of mass arrival per injected mass is defined as the product of the concentration (c) and the pumping rate (Q), divided by the injected mass (M). In Figure 3, the first detection and the time of the peak concentration for RWT precedes that associated with SF_6. Furthermore, cQ/M for the RWT breakthrough curve is approximately an order of magnitude greater than that for SF_6, even though the dilution of RWT from the 2003 test was used to design the mass of SF_6 injected in the 2004 test. In addition, the declining limbs of the two breakthrough curves shown in Figure 3 are different. The breakthrough curve for SF_6 shows a more elongated tail than that for RWT. The breakthrough curve for RWT was truncated after approximately 12.75 h, so the complete history of the declining limb of the breakthrough curve is not available. In the following section, the possible causes for the differences in the breakthrough curves for RWT and SF_6 in Figure 3 are discussed.

4.1. Chemical Diffusion

[28] The difference between the first detection and peak associated with RWT and SF_6 can be attributed to the different free-water diffusion coefficients for RWT and SF_6. The free-water diffusion coefficient for SF_6 [*Cook and Herczeg*, 2000] is approximately an order of magnitude greater than the free-water diffusion coefficient for fluorescent tracers [see, e.g., *Sabatini*, 2000], such as RWT. The magnitude of the free-water diffusion coefficients for the tracers would affect the mass exchange between the mobile groundwater in the touching-vug flow zones and immobile groundwater contained within the interparticle and separate-vug porosity.

[29] To examine the effect of chemical diffusion on the migration of RWT and SF_6 under conditions similar to those of the tracer tests in the Biscayne aquifer, simulations were conducted for the one-dimensional transport of a nonreactive tracer subject to advection and dispersion in a mobile fluid phase (e.g., the touching-vug porosity), with diffusion into an immobile fluid phase (e.g., the interparticle and separate-vug porosity). Several researchers have found that a one-dimensional, linear flow regime can adequately describe chemical transport in a convergent flow regime in fractured rock, because of the "channeling" of flow in fractures and other highly permeable features [see, e.g., *Raven et al.*, 1988; *Maloszewski and Zuber*, 1993]. In reality, because of heterogeneity, the characteristics of the flow regime are likely to lie between linear and radial conditions; a linear flow regime is used here to illustrate the role of chemical diffusion for tracers with different free-water diffusion coefficients. In the simulations, the free-water diffusion coefficients for the tracers are chosen to be similar to those of RWT and SF_6, and the travel distance,

Table 2. Parameters Used in One-Dimensional Simulations of Tracer Migration[a]

Parameter	Value	Source of Information
Distance down gradient from injection location for detection of breakthrough curve, X (m)	100	Approximate distance between injection (G-3817) and pumped (S-3164) wells
Mobile fluid phase porosity, n_m	0.4	Porosity of touching-vug flow zone from *Renken et al.* [2008]
Immobile fluid phase porosity, n_I	0.2	Porosity of interparticle and separate-vug porosity from *Cunningham et al.* [2006]
Velocity, mobile fluid phase, v_m (m/d)	480	Approximate velocity based on first detection of SF_6 at pumped well
Dispersivity, mobile fluid phase, α (m)	2	Interpretation of tracer test from *Renken et al.* [2008]
Duration of pulse injection, t_p, (days)	0.042	Approximate duration of tracer injection and flushing with tracer-free water in February 2004 tracer test
Formation factor, β	0.1	*Ohlsson and Neretnieks* [1995]
Order of magnitude estimate of the free-water diffusion coefficient for SF_6, D_w (m^2/d)	10^{-4}	*Cook and Herczeg* [2000]
Order of magnitude estimate of the free-water diffusion coefficient for RWT, D_w (m^2/d)	10^{-5}	*Sabatini* [2000]

[a]Here m is meters; m/d is meters per day; dispersion of the mobile fluid phase is calculated as $D_m = \alpha v_m$; values of specific surface area of mobile fluid phase, S_m, and the effective diffusion coefficient in the immobile fluid phase, D_i, are shown in Figure 4.

velocity, and dispersion are chosen to be similar to conditions associated with the tracer tests.

[30] The equations describing the one-dimensional transport of a nonreactive tracer in the mobile and immobile fluid phases are as follows [*Shapiro*, 2001]:

$$n_m \frac{\partial c_m}{\partial t} + n_m v_m \frac{\partial c_m}{\partial x} - n_m D_m \frac{\partial^2 c_m}{\partial x^2} = S_m \left[n_i D_i \frac{\partial c_i(z,t;x)}{\partial z}\bigg|_{z=0} \right] \quad (1)$$

$$n_i \frac{\partial c_i}{\partial t} - n_i D_i \frac{\partial^2 c_i}{\partial z^2} = 0 \quad (2)$$

where c_m and c_i are the concentrations in the mobile and immobile fluid phases, respectively, n_m and n_i are the porosities associated with the mobile and immobile fluid phases, respectively, v_m is the fluid velocity in the mobile fluid phase, D_m is the dispersion in the mobile fluid phase, which is assumed to be the product of the fluid velocity and the dispersivity, α, S_m is the specific surface area defined as the surface area of the mobile fluid phase per unit volume, $D_i = \beta D_w$ is the effective diffusion coefficient in the immobile fluid phase, which is the product of the free-water diffusion coefficient for the tracer under consideration, D_w, and a formation factor, β, that reduces the magnitude of the free-water diffusion because of the tortuosity of the void space in the immobile fluid phase [*Shapiro*, 2001], t is time, x is the distance along the orientation of the one-dimensional flow regime, and z is the distance into the medium containing the immobile fluid phase. The term on the right-hand side of (1) defines the mass exchange between the mobile and immobile fluid phases, which is proportional to the concentration gradient in the immobile fluid phase at the contact between the mobile and immobile fluid phases ($z = 0$).

[31] The boundary and initial conditions for (1) are

$$c_m(x = 0, 0 \le t \le t_p) = C_0; \qquad c_m(x = 0, t \ge t_p) = 0 \quad (3)$$

$$\frac{\partial c_m}{\partial x}(x \to \infty, t) = 0 \quad (4)$$

$$c_m(x, t = 0) = 0 \quad (5)$$

where C_0 is the concentration of the injected tracer solution, and t_p is the duration of the pulse injection of the tracer solution. Equation (3) defines the duration of the pulse injection of the tracer solution at $x = 0$, (4) states that there is no change in the concentration gradient at large distances from the injection location, and (5) denotes that there is no tracer mass in the mobile fluid phase prior to the tracer injection.

[32] The boundary and initial conditions for (2) are

$$c_i(z = 0, t; x) = c_m(x, t) \quad (6)$$

$$\frac{\partial c_i}{\partial z}(z \to \infty, t; x) = 0 \quad (7)$$

$$c_i(z, t = 0; x) = 0 \quad (8)$$

Equation (6) defines the equivalence in the concentration at the contact between the mobile and immobile fluid phases, (7) states that there are no changes in the concentration gradient at large distances from the contact between the mobile and immobile fluid phases, and (8) states that there is no tracer mass in the immobile fluid phase prior to the tracer injection.

[33] Equations (1)–(8) consider a continuum interpretation of the mobile fluid phase. Similar equations have been developed for chemical transport in discrete fractures [see, e.g., *Tang et al.*, 1981]. A continuum interpretation is considered here because the touching-vug porosity is characterized as dissolution-enhanced, interconnected, and tortuous burrows [*Renken et al.*, 2008], rather than a single, areally extensive planar feature. In addition, the mathematical development given above assumes that dispersion arising from sampling from the borehole is insignificant, where the pumping rate in the production well is large relative to volume of fluid in the borehole. The values of the parameters used in the simulations are given in Table 2, along with the

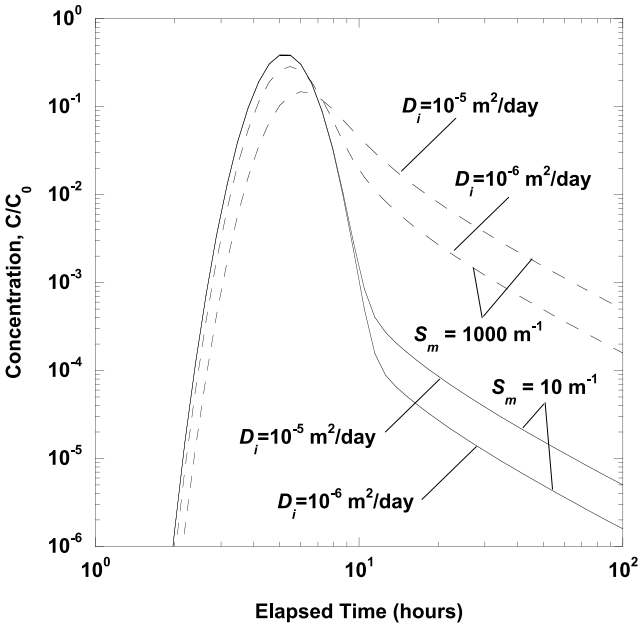

Figure 4. The results of simulations of the concentration at 100 m down gradient from an injection location for two tracers with free-water diffusion coefficients that differ by an order of magnitude and are subject to advection, dispersion, and matrix diffusion in a formation, where the specific surface of the mobile fluid phase, S_m, is equal to 10 m^{-1} and 1000 m^{-1}. Physical parameters for the simulations are given in Table 2.

source of information. Equations (1)–(8) are solved by taking the Laplace transformation and numerically inverting the Laplace transform solution [see, e.g., *Barker*, 1982].

[34] Breakthrough curves for tracers with different diffusion coefficients were simulated with $S_m = 10$ m^{-1} (Figure 4). For this value of S_m, there is no noticeable difference in the first arrival or peak concentration for the two tracers. Differences in the breakthrough curves arise at late times. The tracer with the larger diffusion coefficient preferentially diffuses into the immobile fluid phase, resulting in a slightly smaller peak concentration (for the tracer with the larger diffusion coefficient). As the pulse of the tracer solution migrates in the mobile fluid phase, the tracer diffuses into the immobile fluid phase. After the tracer pulse has been advected down gradient, concentration gradients are conducive for the tracer mass in the immobile fluid phase to diffuse back into the mobile fluid phase and be subject to advection and dispersion. This yields the elongated tails associated the breakthrough curves (Figure 4). The tracer with the larger diffusion coefficient exhibits a more elongated tail when compared with the tracer with the smaller diffusion coefficient, because more of that tracer has diffused into the immobile fluid phase, and it is subsequently delayed in its migration down gradient. For this conceptualization of diffusion into the immobile fluid phase, the tails of both breakthrough curves have the same slope on the log-log plot of concentration versus time (Figure 4), where the slope equals −1.5 [see, e.g., *Moench*, 1995; *Becker and Shapiro*, 2000].

[35] Larger values of S_m result in noticeable differences in the first arrival and the time of the peak concentration for tracers with free-water diffusion coefficients that differ by an order of magnitude (Figure 4). The movement of a tracer solution with the larger diffusion coefficient appears as if it is slightly retarded relative to the tracer with the smaller diffusion coefficient. Again, at late times, the breakthrough curves exhibit a separation, with the tracer having the larger diffusion coefficient exhibiting a more elongated declining limb, and the tails of the two breakthrough curves have a slope of −1.5 on a log-log plot of concentration versus time.

[36] An order of magnitude difference in the free-water diffusion coefficients associated with RWT and SF_6 can explain the offset in the experimental breakthrough curves shown in Figure 3, provided that the specific surface area, S_m, is sufficiently large. The nature of the touching-vug porosity in the Biscayne aquifer as described by *Cunningham et al.* [2006] is likely to have considerable surface area for diffusion because of the numerous interconnected burrows that form the touching-vug void space; currently, there are no independent estimates of S_m associated with the touching-vug flow zones in the Biscayne aquifer. The magnitude of S_m used in the simulations shown in Figure 4 is presented for illustrative purposes to demonstrate the effect of chemical diffusion on the results of tracers with different free-water diffusion coefficients. Bounds on S_m cannot be identified because S_m is scaled by the formation factor, β, and the matrix porosity, n_i, and the values of these parameters for the Biscayne aquifer are not known with great certainty.

[37] In Figure 4, for the larger value of S_m, the tracer with the larger diffusion coefficient has a concentration that is considerably less than the tracer with the smaller diffusion coefficient at comparable times prior to the peak concentration. The difference in the concentrations of the two breakthrough curves shown in Figure 4 (for $S_m = 1000$ m^{-1}) is analogous to the difference between cQ/M for RWT and SF_6 shown in Figure 3; SF_6 has a rate of mass arrival approximately an order of magnitude less than that of RWT. The effect of chemical diffusion could also explain the low concentrations of halon-1211 that were obtained in the 2004 tracer test. The masses of halon-1211 and SF_6 injected into the formation were designed from the rate of mass arrival per injected mass for RWT observed in the 2003 tracer test. The free-water diffusion coefficient associated with halon-1211 [*Cook and Herczeg*, 2000], coupled with a large specific surface of the mobile fluid phase, could have resulted in concentrations of halon-1211 that were above the detection limit of the gas chromatography only during the time associated the peak of the breakthrough curve; this rendered the response for halon-1211 at the production well uninterpretable in the 2004 test. In addition, the effect of gas stripping during sampling as a factor in the concentrations of halon-1211 and SF_6 is discounted because different methods of collecting water samples for analyses of halon-1211 and SF_6 were employed, and it would be fortuitous that gas stripping affected both of these methods of sample collection in a similar manner.

[38] Assuming equilibrium conditions between the head space in the injection tank and the gas in the injection solution could yield an overestimate of the mass of SF_6 injected into the formation. Assuming a smaller injected mass of SF_6 would yield larger values of cQ/M for SF_6 in Figure 3, but it would not explain the slight delay in the arrival of SF_6 relative to RWT, and the general character of the declining limb of the SF_6 breakthrough curve would not

change. The difference in the free-water diffusion coefficients for SF_6 and RWT, however, can explain the offset in this breakthrough curves, and additional confidence in the mass of SF_6 injected would constrain the magnitude of S_m.

4.2. Slow Advection

[39] The simulations of tracer migration through mobile and immobile fluid phases in Figure 4 exhibited declining limbs of the breakthrough curves that were controlled by chemical diffusion. When the simulated breakthrough curves are shown as log-log plots of concentration versus time, the declining limb of the breakthrough curves appear as straight lines with a slope of −1.5 (Figure 4). For one-dimensional diffusion into the immobile fluid phase, the slope of the declining limb of the breakthrough curve is the same regardless of the magnitude of the free-water diffusion coefficients of the tracers. Tracer tests conducted by *Garnier et al.* [1985] in a chalk aquifer showed similar results to those in Figure 4 for tracers with different free-water diffusion coefficients [*Moench*, 1995].

[40] In contrast to the results of *Garnier et al.* [1985], *Becker and Shapiro* [2000] conducted weak dipole and convergent tracer tests in a fractured crystalline rock, using tracers with different free-water diffusion coefficients, where the breakthrough curves showed no separation in their declining limbs [*Becker and Shapiro*, 2000]. In addition, the declining limbs of the breakthrough curves exhibited straight-line slopes of −2 on log-log plots of concentration versus time. *Becker and Shapiro* [2000, 2003] attributed the slope of −2 and the lack of separation of the declining limbs of the breakthrough curves to "slow advection." In the geologic setting considered by *Becker and Shapiro* [2000], the hydraulic conductivity of fractures ranged over more than 6 orders of magnitude. Therefore, tracers migrating through the fractures experience variability in the velocity over many orders of magnitude. The fastest velocity flow paths control the first detection and the peak concentration, whereas the slowest velocity flow paths control the declining limb of the breakthrough curves.

[41] The declining limbs of breakthrough curves from pulse injection tracer tests that exhibit straight lines on log-log plots of concentration versus time are usually attributed to chemical diffusion. In formations having a wide range in the fluid velocity, the slowest velocities can give rise to a process analogous to chemical diffusion. For example, consider part of a tracer solution that migrates from a high-velocity flow path to a low-velocity flow path, and then reemerges into a high-velocity flow path, where water samples are collected for the analysis of the tracer solution. The tracer solution in the low-velocity flow path has migrated a short distance over an extended period of time, which is analogous to diffusion into and out of an immobile fluid phase [see, e.g., *Coats and Smith*, 1964]. In the case of diffusion into and out of an immobile fluid phase, no distance is traversed by the tracer, whereas for slow advection, the advected distance is nonzero but small. Under the circumstances of slow advection, chemical diffusion into and out of the porous matrix of an intact rock is still ongoing, however, the magnitude of that process is dwarfed by the apparent diffusion resulting from the advection through low-velocity flow paths. *Becker and Shapiro* [2003] demonstrated that the superposition of multiple breakthrough curves, each being subject to advection and dispersion, yields a cumulative breakthrough curve with a linear slope of the declining limb equal to −2 on a log-log plot of concentration versus time, provided that there is a wide range in the fluid velocity associated with the various flow paths.

[42] The phenomenon of slow advection as hypothesized by *Becker and Shapiro* [2000, 2003] and *Shapiro* [2001] is not contradictory to the results of *Garnier et al.* [1985]. The results of *Garnier et al.* [1985] can be considered as one extreme, where (1) fluid velocity in the mobile fluid phase does not range over several orders of magnitude, (2) variability in the fluid velocity can be incorporated into a Fickian interpretation of dispersion, and (3) chemical diffusion dominates the tail of a pulse injection tracer experiment. The results of *Becker and Shapiro* [2000] could be considered another end-member, where there is large variability in the fluid velocity that cannot be characterized by a Fickian interpretation of dispersion, and slow advection dominates the declining limbs of pulse injection tracer experiments. It is conceivable, that a continuum of responses between these end-members could be realized in heterogeneous subsurface settings.

[43] The tracer test conducted in the Biscayne aquifer in 2003 using RWT was prematurely terminated, and the characteristics of the declining limb of the breakthrough curve for that test on a log-log plot of cQ/M versus time cannot be definitively identified (Figure 5). A log-log plot of cQ/M versus time for SF_6 in the 2004 tracer test is shown in Figure 5. From approximately 30 h of elapsed time until SF_6 samples were below the analytical detection limit at an elapsed time of approximately 164 h, the slope of the SF_6 breakthrough curve is approximately equal to −2.0. A trend line is shown on Figure 5, which is a minimization of the squared residuals between a straight line and the SF_6 data

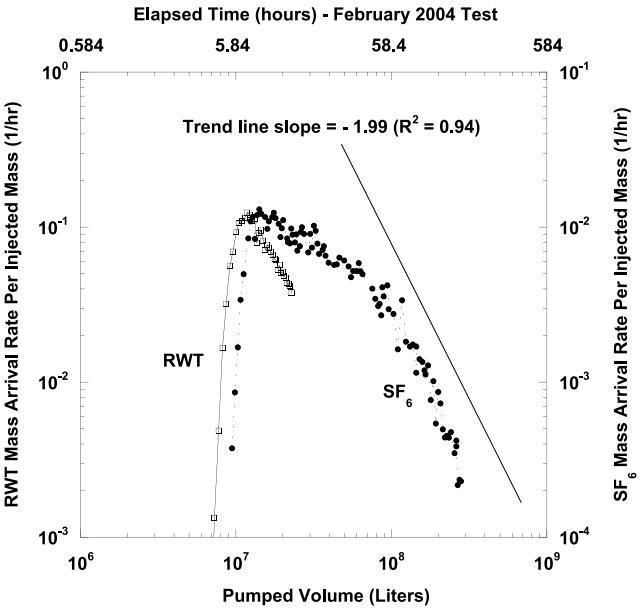

Figure 5. The logarithm of concentrations of RWT from the April 2003 tracer test [*Renken et al.*, 2008] and SF_6 from the February 2004 tracer test at the tracer recovery well, S-3164, plotted as a function of the logarithm of the pumped volume at the tracer recovery well.

from approximately 30 to 164 h of elapsed time. The slope of the best fit straight line is −1.99 with a correlation coefficient of $R^2 = 0.94$.

[44] The slope of −2 on the breakthrough curve for SF_6 implies that the transport in the touching-vug flow zones, where the tracer was introduced in the Biscayne aquifer, may be controlled by multiple pathways having fluid velocities that range over several orders of magnitude. The multiple flow paths in the karst limestone of the Biscayne aquifer could be analogous to the channeling encountered in fractures due to slight variations in fracture aperture [*Neretnieks et al.*, 1982]. Slight variations in the size of dissolution-enhanced and interconnected burrow holes within the touching-vug flow zones in the Biscayne aquifer could yield multiple flow paths with a wide range of velocities. Chemical diffusion is still assumed to be present during the declining limb of the SF_6 breakthrough curve, however, the diffusion into and out of the interparticle and separate-vug porosity adjacent to the touching-vug flow zones is assumed to be dwarfed by the phenomenon of slow advection.

[45] Figure 6 shows the results of superimposing multiple dimensionless breakthrough curves subject to advection, dispersion, and matrix diffusion, where the advection associated with the individual breakthrough curves varies over more than an order of magnitude. The breakthrough curves were generated using the transfer function developed by *Becker* [1996] and applied in *Becker and Shapiro* [2003], where it is assumed that the velocity of the flow paths varies as a function of the square of the aperture of the flow path, and the mass flux varies as the cube of the aperture of the flow path [*Becker and Shapiro*, 2003]. Similar to Figure 4, a linear flow regime is applied in the simulations shown in Figure 6, and the velocities for the flow paths are chosen from a uniform distribution. Following the peak of the cumulative breakthrough curve for the rate of mass arrival in Figure 6, the declining limb of the cumulative breakthrough curve exhibits a slope of −2. At later times, however, the declining limb of the cumulative breakthrough curve transitions to a slope of −1.5, because the individual breakthrough curves each exhibit the effects of chemical diffusion at later times (with slope of −1.5). The parameters of the simulation in Figure 6 were chosen so that the individual breakthrough curves were not dominated by chemical diffusion at times immediately following the peak concentration.

[46] It should be noted that the entire extent of the declining limb of the log-log plot of the breakthrough curve for SF_6 does not exhibit a constant slope equal to −2 (Figure 5). From the time of the peak concentration at 8.25 h to approximately 30 h, the breakthrough curve for SF_6 displays a slight monotonic decline in the rate of mass arrival, but this portion of the breakthrough curve does not exhibit the steep declining limb associated with the later part of the breakthrough curve. If it is hypothesized that the SF_6 breakthrough curve is the superposition of the breakthrough curves from multiple flow paths with different velocity, it is plausible that the slight monotonic decline in the rate of mass arrival for SF_6 from 8.25 to 30 h of elapsed time is representative of the distribution of the fluid velocity in the flow paths within the formation. The slight monotonic decline in the rate of mass arrival for SF_6 from 8.25 to 30 h could be the result of multiple flow paths of a similar velocity, rather than a uniform distribution of velocity used in Figure 6. *Becker and Shapiro* [2003] proposed that the tracer mass carried by flow paths is proportional to the volumetric flow rate associated with each flow path. *Becker and Shapiro* [2003] considered fracture aperture as the geometric factor controlling the fluid velocity, volumetric flow rate, and the mass flux in each flow path. In the touching-vug flow zones of the Biscayne aquifer, channels of a given aperture could also be hypothesized to represent the interconnected touching-vug porosity to arrive at analogous relationships between the fluid velocity, volumetric flow rate, and mass flux.

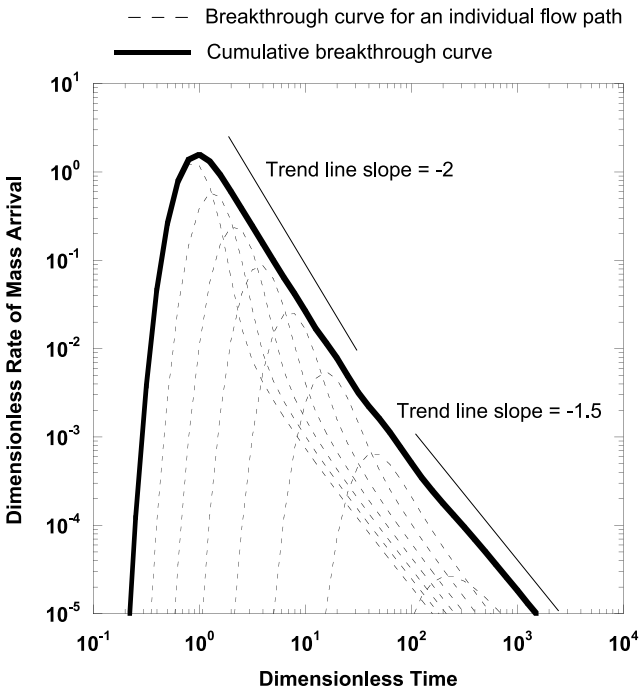

Figure 6. The logarithm of the dimensionless rate of mass arrival versus the logarithm of the dimensionless time for individual linear flow paths subject to advection, dispersion, and matrix diffusion, and the cumulative breakthrough curve for all flow paths.

5. Summary and Conclusions

[47] A converging flow regime tracer test using a nonreactive tracer was conducted in the Biscayne aquifer in southeastern Florida in February 2004. The Biscayne aquifer is a highly transmissive, karst limestone that is characterized by areally extensive intervals of touching-vug porosity that are responsible for transmitting most of the groundwater in the limestone. The touching-vug flow zones are separated by less transmissive intervals of interparticle and separate-vug porosity that provide aquifer storage [*Renken et al.*, 2008].

[48] The tracer test was conducted by injecting a solution containing SF_6 into touching-vug flow zones that were isolated in a borehole approximately 97 m from a production well (pumping at approximately 476 L/s) that served as the location of the tracer recovery. The injection of the tracer solution was followed by the injection of tracer-free

water to force the tracer out of the injection borehole and into the formation. The breakthrough curve for SF_6 at the production well showed a rapid breakthrough with the first detection of the tracer at approximately 5 h, and the peak concentration at approximately 8 h. In spite of the highly transmissive nature of the Biscayne aquifer, SF_6 was not rapidly flushed through the aquifer. The concentration for SF_6 showed an elongated tail, where SF_6 was detected for approximately 6 d after the tracer injection, and only 42% of the tracer mass was recovered at the production well. At approximately 160 h after the tracer injection, the concentration of SF_6 in water samples was below the detection limit of the gas chromatograph used for the analysis of SF_6. It is likely that SF_6 was still being withdrawn from the production well after 160 h, thus the tail of the breakthrough curve is likely to have extended well beyond the termination of the collection of water samples.

[49] The extended retention of SF_6 in the formation after the tracer injection is attributed to a combination of chemical diffusion and slow advection. After the tracer injection, the tracer diffuses from the water in the touching-vug flow zones to the water in the interparticle porosity because of chemical gradients. After the pulse of the SF_6 mass has been advected down gradient, concentration gradients in the interparticle porosity are conducive for the tracer to diffuse back into the touching-vug flow zones and be subject to advection and dispersion. Because of the magnitude of the free-water diffusion coefficient for SF_6 and the surface area of the limestone in the touching-vug flow zones through which SF_6 can diffuse, the first detection and the peak of the SF_6 breakthrough curve appears to be slightly retarded in comparison to tracers with smaller free-water diffusion coefficients. The results of the tracer test conducted in the Biscayne aquifer in April 2003 and described by *Renken et al.* [2008] was used in this comparison. The tracer test conducted in April 2003 used RWT as a tracer, where RWT has a free-water diffusion coefficient that is approximately an order of magnitude smaller than that of SF_6.

[50] Chemical diffusion into an immobile fluid phase, such as the interparticle porosity of the Biscayne aquifer, will result in elongated tails in breakthrough curves with a declining limb having a straight line on log-log plots of concentration versus time. Usually, a straight line on the declining limb of a breakthrough curve is attributed to chemical diffusion. Chemical diffusion, however, should give rise to a slope of the tail of the breakthrough curve equal to -1.5. The slope of -2 in breakthrough curve for SF_6 in the Biscayne aquifer is attributed to the process of slow advection. It is hypothesized that the touching-vug flow zones in the Biscayne aquifer have multiple flow paths that exhibit a wide range in the fluid velocity. Usually, variability of the fluid velocity is conceptualized in hydrodynamic dispersion; however, in heterogeneous geologic settings, such as the karst limestone of the Biscayne aquifer, the large variability in the fluid velocity cannot be incorporated into a Fickian interpretation of hydrodynamic dispersion. The slowest velocity flow paths give rise to an elongated tail in the breakthrough curve that resembles a diffusive process, but is an artifact of large variations in the fluid advection.

[51] The pumping rate associated with the production well, where the tracer test in the Biscayne aquifer was conducted, is likely to result in turbulent flow conditions. Turbulent flow could result in eddies in the flow regime through the touching-vug porosity that could give rise to chemical retention of the tracer solution. Chemical exchange between turbulent eddies and flow paths in the Biscayne could be a time-dependent process that behaves analogously to diffusion. Additional investigations on the effect of turbulence on chemical transport in karst formations are needed to understand this relationship. It should be noted, however, that breakthrough curves similar to that of SF_6 in the Biscayne aquifer have also been seen in other geologic settings, where turbulent conditions are unlikely [see, e.g., *Becker and Shapiro*, 2000].

[52] The retention of the tracer mass in the interparticle porosity and slow flow paths in the Biscayne aquifer indicates that contaminants introduced into the groundwater are likely to experience a significant longevity. For the test conducted in this investigation, a tracer solution was injected into the formation over a period of approximately 1 h. The breakthrough curve for the tracer at a pumping well approximately 100 m away from the injection location showed elongated breakthrough tailing that extended over approximately 6 days. After 6 days the tracer was no longer detected; however, this was the result of the tracer concentration declining below the detection limit. During the first 6 d of the tracer test only 42% of the tracer mass was recovered, indicating that a significant amount of the tracer mass was still resident in the formation at the termination of the test. Contamination events extending over days, weeks, or months in the Biscayne aquifer could lead to the degradation of water quality ranging from years to tens of years or more.

[53] **Acknowledgments.** The authors acknowledge the support of the Miami-Dade County Department of Environmental Resource Management (DERM) and Water and Sewer Department (WASD), the American Water Works Research Foundation, and the U.S. Geological Survey (USGS) National Research Program in conducting this investigation. The authors also acknowledge the contributions of Eurybiades Busenberg (USGS) for the preparation of the dissolved gases and the analyses of SF_6 and halon-1211 and Tyler Coplen (USGS) for the analysis of ^2H. Peggy Widman (USGS) provided support in sample preparation. The authors are also grateful for the assistance in sample collection and field operations provided by Kevin Cunningham, Marc Stewart, Alyssa Dausman, Mike Wacker, and Dawn Edwards of the USGS, Julie Baker and Hillol Guha of Miami-Dade DERM, and Clint Oakley of Miami-Dade WASD and other county staff. Leonard F. Konikow and Charles J. Taylor of the USGS and Nico Goldscheider are acknowledged for their comments in improving the manuscript, as are Scott Tyler and the anonymous reviewers.

References

Barker, J. A. (1982), Laplace transform solutions for solute transport in fissured aquifers, *Adv. Water Resour.*, *5*, 98–104, doi:10.1016/0309-1708(82)90051-3.

Becker, M. W. (1996), Tracer tests in a fractured rock and their first passage time mathematical models, Ph.D. thesis, 210 pp., Univ. of Tex. at Austin, Austin.

Becker, M. W., and A. M. Shapiro (2000), Tracer transport in crystalline fractured rock: Evidence of non-diffusive breakthrough tailing, *Water Resour. Res.*, *36*(7), 1677–1686, doi:10.1029/2000WR900080.

Becker, M. W., and A. M. Shapiro (2003), Interpreting tracer breakthrough tailing from different forced-gradient tracer experiment configurations in fractured bedrock, *Water Resour. Res.*, *39*(1), 1024, doi:10.1029/2001WR001190.

Birgersson, L., and I. Neretnieks (1990), Diffusion in the matrix of granitic rock: Field test in the Stripa Mine, *Water Resour. Res.*, *26*(11), 2833–2842, doi:10.1029/90WR00822.

Bullister, J. L., D. P. Wisegarver, and F. A. Menzia (2002), The solubility of sulfur hexafluoride in water and seawater, *Deep Sea Res., Part I*, *49*, 175–187.

Busenberg, E., and L. N. Plummer (2000), Dating young groundwater with sulfur hexafluoride: Natural and anthropogenic sources of sulfur hexafluoride, *Water Resour. Res.*, *36*(10), 3011–3030, doi:10.1029/2000WR900151.

Coats, K. H., and B. D. Smith (1964), Dead-end pore volume and dispersion in porous media, *SPEJ Soc. Pet. Eng. J.*, *4*, 73–84, doi:10.2118/647-PA.

Cook, P., and A. L. Herczeg (Eds.) (2000), *Environmental Tracers in Subsurface Hydrology*, 529 pp., Kluwer Acad., Boston, Mass.

Cunningham, K. J., M. A. Wacker, E. Robinson, J. F. Dixon, and G. L. Wingard (2006), A cyclostratigraphic and borehole geophysical approach to development of a three-dimensional conceptual hydrogeologic model of the karst Biscayne aquifer, southeastern Florida, *U. S. Geol. Surv. Sci. Invest. Rep., 2005-5235*, 69 pp.

Dagan, G. (1984), Solute transport in heterogeneous porous formations, *J. Fluid Mech.*, *145*, 151–177, doi:10.1017/S0022112084002858.

Field, M. S. (1999), The QTRACER program for tracer-breakthrough curve analysis for karst and fractured-rock aquifers, *EPA/600/R-98/156a*, 137 pp., U. S. Environ. Prot. Agency, Washington, D. C.

Field, M. S., and P. F. Pinsky (2000), A two-region nonequilibrium model for solute transport in solution conduits in karstic aquifers, *J. Contam. Hydrol.*, *44*, 329–351, doi:10.1016/S0169-7722(00)00099-1.

Finley, R. J., and N. Tyler (1986), Geological characterization of sandstone reservoirs, in *Reservoir Characterization*, edited by L. W. Lake and H. B. Carroll Jr., pp.1–38, Academic,, Orlando, Fla.

Garnier, J. M., N. Crampon, C. Préaux, G. Porel, and M. Vreulx (1985), Traçage par ^{13}C, ^{2}H, I^{-} et uranine dans la nappe de la craie sénonienne en écoulement radial convergent (Béthune, France), *J. Hydrol.*, *78*, 379–392, doi:10.1016/0022-1694(85)90114-3.

Gelhar, L. J., and C. L. Axness (1983), Three-dimensional stochastic analysis of macrodispersion in aquifers, *Water Resour. Res.*, *19*(1), 161–180, doi:10.1029/WR019i001p00161.

Goldscheider, N. (2005), Fold structure and underground drainage pattern in the alpine karst system Hochifen-Gottesacker, *Eclogae Geol. Helv.*, *98*, 1–17, doi:10.1007/s00015-005-1143-z.

Guswa, A. J., and D. L. Freyberg (2002), On using the equivalent conductivity to characterize solute spreading in environments with low-permeability lenses, *Water Resour. Res.*, *38*(8), 1132, doi:10.1029/2001WR000528.

Haggerty, R., and S. M. Gorelick (1995), Multiple-rate mass transfer for modeling diffusion and surface reactions in media with pore-scale heterogeneity, *Water Resour. Res.*, *31*(10), 2383–2400, doi:10.1029/95WR01583.

Haggerty, R., S. W. Fleming, L. C. Meigs, and S. A. McKenna (2001), Tracer tests in a fractured dolomite: 2. Analysis of mass transfer in single-well injection-withdrawal tests, *Water Resour. Res.*, *37*(5), 1129–1142, doi:10.1029/2000WR900334.

Harvey, R. W., D. W. Metge, A. M. Shapiro, R. A. Renken, C. L. Osborn, J. N. Ryan, K. J. Cunningham, and L. Landkamer (2008), Pathogen and chemical transport in the karst limestone of the Biscayne aquifer: 3. Use of microspheres to estimate the transport potential of *Cryptosporidium parvum* oocysts, *Water Resour. Res.*, *44*, W08431, doi:10.1029/2007WR006060.

Lucia, F. J. (1983), Petrophysical parameters estimated from visual description of carbonate rocks: A field classification of carbonate pore space, *J. Pet. Technol.*, *35*(3), 626–637, doi:10.2118/10073-PA.

Lucia, F. J. (1995), Rock-fabric/petrophysical classification of carbonate pore space for reservoir characterization, *AAPG Bull.*, *79*, 1275–1300.

Mace, R. E., and S. D. Hvorka (2000), Estimating porosity and permeability in a karstic aquifer using core plugs, well tests, and outcrop measurements, in *Groundwater Flow and Contaminant Transport in Carbonate Aquifers*, edited by I. D. Sasowsky and C. M. Wickspp. 93–111, A. A. Balkema, Rotterdam, Netherlands.

Maloszewski, P., and A. Zuber (1991), Influence of matrix diffusion and exchange reactions on radiocarbon ages in fissured carbonate aquifers, *Water Resour. Res.*, *27*(8), 1937–1945, doi:10.1029/91WR01110.

Maloszewski, P., and A. Zuber (1993), Tracer experiments in fractured rocks: Matrix diffusion and the validity of models, *Water Resour. Res.*, *29*(8), 2723–2735, doi:10.1029/93WR00608.

Meigs, L. C., and R. L. Beauheim (2001), Tracer tests in a fractured dolomite: 1. Experimental design and observed tracer recoveries, *Water Resour. Res.*, *37*(5), 1113–1128, doi:10.1029/2000WR900335.

Moench, A. F. (1995), Convergent radial dispersion in a double-porosity aquifer with fracture skin: Analytical solution and application to a field experiment in fractured chalk, *Water Resour. Res.*, *31*(8), 1823–1835, doi:10.1029/95WR01275.

Neretnieks, I., T. Eriksen, and P. Tähtinen (1982), Tracer movement in a single fissure in granitic rock: Some experimental results and their interpretation, *Water Resour. Res.*, *18*(4), 849–858, doi:10.1029/WR018i004p00849.

Neuman, S. P., C. L. Winter, and C. M. Newman (1987), Stochastic theory of field-scale Fickian dispersion in anisotropic porous media, *Water Resour. Res.*, *23*(3), 453–466, doi:10.1029/WR023i003p00453.

Ohlsson, Y., and I. Neretnieks (1995), Literature survey of matrix diffusion theory and of experiments and data including natural analogues, *Tech. Rep. 95-12*, 89 pp., Swed. Nucl. Fuel and Waste Manage. Co., Stockholm.

Parker, B. L., R. W. Gillham, and J. A. Cherry (1994), Diffusive disappearance of immiscible-phase organic liquids in fractured geologic media, *Ground Water*, *32*(5), 805–820, doi:10.1111/j.1745-6584.1994.tb00922.x.

Plummer, L. N., and E. Busenberg (2000), Chlorofluorocarbons, in *Environmental Tracers in Subsurface Hydrology*, edited by P. G. Cook and A. L. Herczeg, pp. 441–478, Kluwer Acad., Boston, Mass.

Quinlan, J. F., and R. O. Ewers (1985), Ground water flow in limestone terranes: Strategy, rationale, and procedure for reliable, efficient monitoring of ground water quality in karst areas, paper presented at 5th National Symposium and Exposition on Aquifer Restoration and Ground Water Monitoring, Natl. Water Well Assoc., Columbus, Ohio.

Quinlan, J. F., and R. O. Ewers (1986), Reliable monitoring in karst terranes: It can be done, but not by an EPA-approved method, *Ground Water Monit. Rev.*, *6*(1), 4–6, doi:10.1111/j.1745-6592.1986.tb01221.x.

Raven, K. G., K. S. Novakowski, and P. A. Lapcevic (1988), Interpretation of field tracer tests of a single fracture using a transient solute storage model, *Water Resour. Res.*, *24*(12), 2019–2032, doi:10.1029/WR024i012p02019.

Renken, R. A., K. J. Cunningham, A. M. Shapiro, R. W. Harvey, M. R. Zygnerski, D. W. Metge, and M. A. Wacker (2008), Pathogen and chemical transport in the karst limestone of the Biscayne aquifer: 1. Revised conceptualization of groundwater flow, *Water Resour. Res.*, *44*, W08429, doi:10.1029/2007WR006058.

Sabatini, D. A. (2000), Sorption and intraparticle diffusion of fluorescent dyes with consolidated aquifer media, *Ground Water*, *38*(5), 651–656, doi:10.1111/j.1745-6584.2000.tb02700.x.

Shapiro, A. M. (2001), Effective matrix diffusion in kilometer-scale transport in fractured crystalline rock, *Water Resour. Res.*, *37*(3), 507–522, doi:10.1029/2000WR900301.

Shapiro, A. M., and P. A. Hsieh (1998), How good are estimates of transmissivity from slug tests in fractured rock?, *Ground Water*, *36*(1), 37–48, doi:10.1111/j.1745-6584.1998.tb01063.x.

Tang, D. H., E. A. Sudicky, and E. O. Frind (1981), Contaminant transport in fractured porous media: Analytical solution for a single fracture, *Water Resour. Res.*, *17*(3), 555–564, doi:10.1029/WR017i003p00555.

Wood, W. W., A. M. Shapiro, P. A. Hsieh, and T. B. Councell (1996), Observational, experimental and inferred evidence for solute diffusion in fractured granite aquifers: Examples from the Mirror Lake watershed, Grafton County, New Hampshire, in *U. S. Geological Survey Toxic Substances Hydrology Program: Proceedings of the Technical Meeting*, vol. 1, edited by D. W. Morganwalp and D. A. Aronson, *U. S. Geol. Surv. Water Resour. Invest. Rep.*, *94-4015*, 167–170.

R. W. Harvey and D. W. Metge, U.S. Geological Survey, 3215 Marine Street, Suite E-127, Boulder, CO 80303, USA.

R. A. Renken and M. R. Zygnerski, U.S. Geological Survey, 3110 SW 9th Street, Fort Lauderdale, FL 33315, USA.

A. M. Shapiro, U.S. Geological Survey, 12201 Sunrise Valley Drive, MS 431, Reston, VA 20192, USA. (ashapiro@usgs.gov)